serval
serveur académique lausannois

Unil
UNIL | Université de Lausanne
Faculty of Biology and Medicine

CHUV

Optical probing of sodium dynamics in neurons and astrocytes

Christophe M. Lamy[1] and Jean-Yves Chatton[1,2]

[1] Department of Cell Biology and Morphology, University of Lausanne, Rue du Bugnon 9, 1005 Lausanne, Switzerland

[2] Cellular Imaging Facility, University of Lausanne, Rue du Bugnon 9, 1005 Lausanne Switzerland

Classification: Biological Sciences - Neuroscience

Corresponding author:

Christophe Lamy

Dept. of Cell Biology and Morphology

University of Lausanne

Rue du Bugnon 9

CH-1005 Lausanne

Switzerland

Tel. +41-21-692-5117

Fax. +41-21-692-5105

E-mail: christophe.lamy@unil.ch

Abstract

Changes in intracellular Na^+ concentration underlie essential neurobiological processes, but few reliable tools exist for their measurement. Here we characterize a new synthetic Na^+-sensitive fluorescent dye, Asante Natrium Green (ANG), with unique properties. This indicator was excitable in the visible spectrum and by two-photon illumination, suffered little photobleaching and located to the cytosol were it remained for long durations without noticeable unwanted effects on basic cell properties. When used in brain tissue, ANG yielded a bright fluorescent signal during physiological Na^+ responses both in neurons and astrocytes. Synchronous electrophysiological and fluorometric recordings showed that ANG produced accurate Na^+ measurement in situ. This new Na^+ indicator opens innovative ways of probing neuronal circuits.

Introduction

The Na^+ concentration gradient across the plasma membrane is essential in maintaining cellular homeostasis. In the nervous system it also drives key processes such as action potential generation, forward and back-propagations, excitatory synaptic transmission and neurotransmitter reuptake. Optical measurements of Na^+ dynamics with fluorescent indicators would thus be a powerful approach to study the function of neural networks with spatial resolution. Thus far however, cellular events behind neuronal activity have been monitored mainly indirectly by Ca^{2+} imaging owing to the comparatively small amplitude of sodium changes occurring during physiological responses and to the lack of satisfactory fluorescent Na^+ indicator (Cossart et al., 2005; Garaschuk et al., 2006a; Gobel and Helmchen, 2007; Kuga et al., 2011; Meier et al., 2006). Unfortunately, Ca^{2+} signals are an indirect reflection of cellular activity. Moreover, the amplitude and kinetics of monitored responses are significantly influenced by the Ca^{2+} buffering effects of both cytosolic proteins and the Ca^{2+} indicator itself (Helmchen et al., 1996; Neher and Augustine, 1992). By contrast Na^+ imaging offers the opportunity to directly and accurately measure a primary component of cell responses with marginal interaction of dye with these responses (Fleidervish et al., 2010).

The most commonly used Na^+-sensitive indicator is sodium-binding benzofuran isophthalate (SBFI) (Lasser-Ross and Ross, 1992; Minta and Tsien, 1989; Rose and Ransom, 1997). This compound requires UV excitation which is suboptimal for imaging deep in tissues due to the strong scattering of UV photons and a high risk of phototoxic damage (Kang et al., 2005). It also precludes simultaneous stimulations by UV-photoactivable caged compounds. In addition, the signal generated with SBFI is much weaker than with the structurally related Ca^{2+} indicator Fura-2 due to a much lower quantum yield and fluorescence change upon Na^+ binding (Minta and Tsien, 1989). Attempts to make a more efficient dye excitable in the visible range did not lead to convincing results. Sodium Green was one noticeable alternative (Szmacinski and Lakowicz, 1997) but it produced inaccurate Na^+ measurements due to interactions with cell proteins (Despa et al., 2000). CoroNa Green, another promising attempt, was disadvantaged by a fast efflux from cells after loading (Meier et al., 2006). Here we describe a novel visible-spectrum Na^+ dye ANG with remarkable characteristics that enables accurate and stable measurements of intracellular Na^+ dynamics in situ during physiological responses.

Materials and methods

Astrocyte culture and dye loading

Cortical astrocytes in primary culture were obtained from 1-3 day-old OF1 and C57BL/6 mice as described previously (Sorg and Magistretti, 1992). Cells were grown at confluency for 3 weeks on glass coverslips in DME medium supplemented with 10% FCS. To load the sodium indicator, astrocyte cultures were incubated in a solution containing (mM): 135 NaCl , 5.4 KCl, 20 HEPES, 1.3 $CaCl_2$, 0.8 $MgSO_4$, 0.78 NaH_2PO_4 , 20 glucose (pH 7.4), supplemented with 0.1% Pluronic F-127 (Molecular Probes), in the presence of 12 μM ANG-AM for 40 min at 37 °C. For imaging, cultures were then transferred to a solution containing (mM): 160 NaCl, 5.4 KCl, 20 HEPES, 1.3 $CaCl_2$, 0.8 $MgSO_4$, 0.78 NaH_2PO_4 , 5 glucose (pH 7.4), bubbled with air and maintained at 37°C.

Brain slice preparation

All experimental procedures were carried out according to the Ordinance on Animal Experimentation. Sprague-Dawley rats (P14-P23) were decapitated and 300 μm tick transverse slices of somatosensory cortex were cut in cold extracellular solution using a vibrating microslicer (VT1000, Leica Microsystems, Heerbrugg). Slices were incubated at 34°C for 1h and then held at room temperature (20–22°C) in extracellular solution until used for recording as described below.

Electrophysiology and dye loading on brain slices

Slices were continuously superfused at a rate of 2 ml/min with an extracellular solution containing (mM): 125 NaCl, 2.5 KCl, 26 $NaHCO_3$, 1.25 NaH_2PO_4, 2 $CaCl_2$ and 1 $MgCl_2$, 10 glucose, bubbled with 95% O_2 and 5% CO_2 and maintained at 34°C. Borosilicate glass pipettes with resistances of 4.0-5.0 MΩ containing (mM): 130 K-gluconate, 5 NaCl, 10 Hepes, 10 phosphocreatine, 2 Mg-ATP, 0.5 Na_2-GTP (adjusted to pH 7.3 with KOH) were used to obtain whole-cell recordings. Signals were amplified using a Multiclamp 700B amplifier (Molecular Devices), filtered at 3 KHz, digitized at 10 KHz using Digidata 1440 (Molecular Devices), and acquired with pClamp 10 electrophysiology package (Molecular devices). In voltage clamp mode, cells were held at -70 mV. For current clamp recording cells were kept with 0 holding current injected. Access resistance and holding current were monitored throughout the

experiments, and data were discarded when these parameters increased beyond 30MΩ or below -30 pA respectively. Intrinsic membrane properties were recorded after a settling time of ≥ 10 min. In experiments coupling electrophysiology with imaging, 200 μM ANG was added to the pipette solution and enough time was allowed for the dye to fill the cell after breaking through. As an alternative we also bulk-loaded the dye by incubating slice with12 μM ANG-AM for 50 min at 37 °C. For the last 20 min of incubation we added 1 μM sulforhodamine 101 (Sigma-Aldrich, St Louis, MO) in order to identify astrocytes.

Stimulation procedures

To generate action currents, depolarizing voltage pulses (80 mV, 2 ms) were applied through the patch pipette. To record dendritic sodium transients, back propagating action potentials were generated by injecting current pulses at the soma (1-4 nA, 2 ms, 50Hz). For experiments requiring local delivery of drugs, a glass pipette of tip diameter 1-2 μm was filled with the drug at diluted the appropriate concentration in extracellular solution, approached at a distance of ~10 μm from the soma and pressure pulses of 10-250 ms, 1-2 psi were applied to the back of the pipette with a Pressure System II (The Toohey Company, Fairfield, NJ) to expel the drug. In cell cultures, drugs were gravity fed to the recording chamber rather than locally applied on individual cells.

Widefield fluorescence imaging

Widefield intracellular imaging was performed on an inverted epifluorescence microscope (Axiovert 100M, Carl Zeiss, Germany) using a 40x 1.3 N.A. oil-immersion objective lens. Fluorescence excitation wavelengths were selected using a monochromator (Till Photonics, Planegg, Germany) and fluorescence was detected using a 12-bit cooled CCD camera (Princeton Instruments, Trenton, NJ). ANG fluorescence was excited at 495nm and detected at >515nm. Excitation spectra were recorded by varying the monochromator settings in the range 380-508nm. Image acquisition was computer-controlled using the software Metafluor (Universal Imaging, Reading, PA). Cells were recorded in a closed thermostated perfusion chamber (Chatton et al., 2000) at 37°C.

For *in situ* calibration, cells were permeabilized for monovalent cations using 6 μg/ml gramicidin and 10 μM monensin with simultaneous inhibition the Na^+/K^+-ATPase using 1 mM ouabain.

Cells were then sequentially perfused with solutions buffered at pH 7.2 with 20mM HEPES and containing 0, 5, 10, 20 and 50mM Na^+, respectively, and 30mM Cl^-, 136mM gluconate with a constant total concentration of Na^+ and K^+ of 165mM.

Confocal imaging

One-photon confocal imaging was performed on living cells on a LSM 510 Meta confocal microscope with a 40x0.8 N.A. water-dipping objective (Carl Zeiss, Jena), with excitation at 488nm, 514 or 543nm. The spectral detector (Meta detector) was used to record dye emission spectra from single cells. Acquisitions of image time series was done either in frame mode (512x512 pixels) at a rate of 1 Hz, or in line-scan mode on a segment of arbitrary length at 500Hz. Synchronization of electrophysiology and imaging was done by means of transistor-transistor logic pulses. To obtain 3 dimensional reconstructions of recorded neurons, z-stacks were acquired with 1μm intervals.

Two-photon imaging

Two-photon imaging was performed on an upright microscope (LSM710 NLO, Carl Zeiss, Jena) using a 20X 1.0 NA water-dipping objective. Femtosecond infrared laser used was from Coherent (Chameleon Ultra II) tunable in the range 690-1040nm. The setup allowed also using one-photon cw Argon laser. A spectral fluorescence detector (Quasar) was used to record emission spectra during one-photon (488nm or 514nm) excitation, or during two-photon excitation (800nm). In other experiments, a non-descanned detector using a 500-550nm bandpass filter was used.

Data analysis

Electrophysiology recording were analyzed with the pClamp 10 software package (Molecular Probes). Peak amplitudes and area under the curve of responses were measured after threshold-based event detection. Wide-field images were processed with the Metafluor (Molecular probes). Confocal and two-photon images were analyzed with Image J (Rasband, W.S., http://rsb.info.nih.gov/ij/). Fluorescence intensity traces were drawn from regions of interest, corrected for background and represented as fractional fluorescence changes (ΔF/F). Three-dimensional reconstructions of neurons from confocal image stacks were performed with Imaris

(Bitplane, Zurich). Further calculations were done with Excel (Microsoft). Charts and curve-fittings were done with Kaleidapgraph (Synergy Software).

Dyes and Drugs

Asante Natrium Green was obtained from TEFLabs, Inc (Austin, TX). ANG-1 AM (Ref# 3500) was used for bulk loading on astrocyte cultures and acute brain slices. ANG-1 TMA+ salt (Ref# 3520) was included to the internal solution for patch-clamp experiments.

Glutamate, AMPA, D-aspartate and ouabain were obtained from Sigma-Aldrich (St Louis, MO), TTX, CNQX and AP5 from Biotrend (Köln), and TFB-TBOA from Tocris Bioscience (Ellisville, MO). They were prepared as stock solution in water, except TFB-TBOA and CNQX that were prepared in DMSO. Final dilution in experimental solutions was 1/1000.

Results

Basic properties the dye

To assess the basic characteristics of the dye, membrane permeable ANG-AM was first loaded in astrocyte primary cultures. Loading was readily achieved (see Material and methods) and led to a bright and homogeneous staining indicating a mainly cytosolic distribution (Fig. 1a). Fluorescent signal was stable over time unlike with some previously available Na^+ dyes (Meier et al., 2006) and suffered very little photobleaching allowing measurements for durations that would typically exceed 1.5h under standard conditions. In situ excitation spectrum recorded on a wide-field microscope showed an excitation maximum at 532nm (Fig. 1b). We then tested whether ANG could be used for experiments on a two-photon microscope. With two-photon illumination, ANG-loaded astrocytes displayed a bright homogeneous fluorescence pattern similar to the one observed with one-photon excitation. Two-photon excitation spectrum extended from 700nm to 890nm with an excitation maximum at 790nm (Fig. 1c). Emission spectrum measured on the spectral detector of a confocal microscope with excitation at 488nm had a maximum at 548nm (Fig. S1). Emission spectra obtained with excitation at 514nm or with two-photon excitation at 800nm were identical to the emission spectrum excited at 488nm (Fig. S1).

Na^+ dependence of indicator fluorescence

We examined the sensitivity of ANG to intracellular Na^+ concentration ($[Na^+]_i$) changes. ANG-loaded astrocytes where perfused with a calibration solution producing a rapid equilibration of sodium across the plasma membrane (Rose and Ransom, 1996). Stepwise increases in $[Na^+]$ were followed by matching increases in ANG fluorescence (Fig. S1). To test whether spectral properties of ANG would change with $[Na^+]$ we repeated the same calibration procedure on a confocal microscope equipped with spectral detection. No shift in the emission spectrum was observed in the range of $[Na^+]$ tested and no isosbestic point was found (Fig. 1d). Peak values of spectra were plotted against corresponding $[Na^+]$ (Fig. 1e). The resulting calibration curve could be fitted by a hyperbolic function with an apparent dissociation constant (K_d) of 38.7mM, in the upper range of expected $[Na^+]_i$ values. In addition, Na^+-dependence of ANG fluorescence was fairly proportional to $[Na^+]_i$ in the 0-20mM range with a $\Delta F/F$ of 50 % corresponding to a change in $[Na^+]_i$ of 10.5mM indicating a higher sensitivity for detection of Na^+ than existing Na^+ probes (Meier et al., 2006). We then verified that ANG could detect stereotypic cytosolic Na^+ changes

produced by pharmacological stimulations. Glutamate and ouabain applications to ANG-filled astrocytes induced fluorescence increases reflecting the activation of Na^+-coupled glutamate transporters and inhibition of Na^+/K^+ ATPase respectively, as described earlier (Chatton et al., 2000).

Physiological Na^+ responses in neurons

To further analyze ANG functional properties, we tested its Na^+ sensitivity in rat brain slices. To this purpose we patched layer 2/3 pyramidal neurons in somatosensory cortex with a pipette solution containing ANG and then performed simultaneous whole-cell patch clamp recordings and ANG fluorescence measurements (Fig. 2a and Material and methods). Intrinsic membrane properties of ANG-filled neurons were not altered when compared to control cells patched in the same conditions with an ANG-free pipette solution (Table 1). We stimulated neurons by trains of short depolarizing pulses applied through the patch pipette. Depolarizing steps induced fast Na^+ action currents (ACs) and simultaneous transient increases in ANG fluorescence at the soma that were repeatable and could be blocked by tetrodotoxin (TTX) (Fig. 2b). Trains of as little as 10 ACs could be reliably detected. Repeated AC trains resulted in proportional increases in Na^+ transient amplitude (Fig. 2b,c, n=4). We estimated from the Na^+ calibration curve that 1 AC would result in an increase of 0.1 %$\Delta F/F$ and 21μM $[Na^+]_i$.

Fast Na^+ changes typically found in small cellular compartments are usually of higher amplitude than those observed at the soma (Fleidervish et al., 2010; Rose et al., 1999). To see whether ANG could reliably detect such events we measured fluorescence changes in the apical dendrite of layer 2/3 pyramidal while simultaneously delivering trains of action potentials (APs) through a patch pipette at the soma (Fig. 2d). This procedure was shown to result in dendritic Na^+ spikes induced by the backpropagation of APs (Jaffe et al., 1992; Stuart and Sakmann, 1994). Fast increases in ANG fluorescence were observed at 20 to 50μm from the soma during trains of 10 and 20 APs (Fig. 2e). Average amplitude of response to 10 APs was 33.5$\pm$2.6%$\Delta F/F$ (n=10) equivalent to a rise of 7 mM in $[Na^+]_i$ and increased significantly with a stimulus train of 20 APs (33.5$\pm$2.6 vs. 41.5$\pm$2.1 %$\Delta F/F$, n=10, 2 sided t-test, p=0.004; Fig. 2f).

Reliability of Na^+ measurements

To further check the accuracy of $[Na^+]_i$ measurements with ANG in the brain slice preparation we puffed 2-amino-3-(5-methyl-3-oxo-1,2-oxazol-4-yl) propanoic acid (AMPA) next to the soma of patched layer 2/3 cortical pyramidal cells. AMPA puffs resulted in typical Na^+-driven inward currents that paired with simultaneous ANG fluorescence increases. Both were almost totally blocked by AMPA antagonist 6-cyano-7-nitroquinoxaline-2,3-dione (CNQX) (Fig. 2g,h) and partially recovered after drug washout (Fig. 2h). Graded increases in AMPA puff duration resulted in a proportional increase in AMPA current amplitude and a matching increase in ANG transient amplitude (Fig. 2g,h, n=4 cells). Individual ANG fluorescence values were plotted against corresponding AMPA current amplitudes and fit by a simple linear regression (slope=2.8 %ΔF/F/nA, r=0.88, n=49 events) (Fig. 2i). Similarly, fluorescence response correlated well with AMPA-dependent total charge transfer (r=0.83) with a slope of 3.1%ΔF/F/nC corresponding to a $\Delta[Na^+]_i$/charge ratio of 0.65 mM/nC according to ANG calibration data. We then measured the somatic volume of recorded cells from confocal image stacks and calculated that AMPA currents would produce a $\Delta[Na^+]i$ of 0.87mM/nC.

Astrocytic Na+ responses

Finally we tested bulk-loading of ANG in brain slices. Incubation of neocortical slices with ANG-AM at physiological temperature resulted in a selective loading of astrocytes as shown by the colocalization of the dye with astrocyte-selective sulforhodamine 101 labeling (Nimmerjahn et al., 2004) (Fig. 3a). Puffs of glutamate applied next to astrocytes induced fluorescence transients as expected from the activation of Na^+-coupled glutamate transporters (Chatton et al., 2000) (Fig. 3b). The change in fluorescence was linearly related to the puff duration and was decreased to 60.1±8.7% of control (p=0.003, 2-sided t-test, n=6) by glutamate transporter competitive inhibitor TFB-TBOA (100nM) (Fig. 3c, Fig. S2). Similarly, Na^+-coupled excitatory aminoacid transporters activation by D-aspartate (200μM) induced a 2.0% (n=6) increase in fluorescence (Fig. S2). No change in fluorescence was seen after application of excitatory synaptic transmission inhibitors CNQX and AP5, pointing to a direct effect of glutamate on astrocytes (Fig. S2).

Discussion

This study reports on the performance of ANG, a novel synthetic dye, for fluorescent imaging of Na^+ variations in live biological samples and assesses its usefulness for optical probing of brain function.

We first tested the loading of the acetoxymethyl ester-conjugated, membrane-permeant form of the dye in primary astrocyte cultures. The flat shape of astrocytes in monolayer cultures makes it easy to monitor cell loading with the dye and the partitioning of the molecule in subcellular compartments. Cells were filled with high concentrations of dye by using standard loading procedures in contrast with previously tested Na^+ indicator Sodium Green. Distribution of the dye was largely cytosolic. No subcellular organelles seemed to significantly take up this indicator unlike previous molecules of the same family or mitochondria-targeting Na^+ indicator CoroNa Red (Bernardinelli et al., 2006). When ANG-AM was removed from extracellular medium, cells remained loaded with ANG allowing stable long-lasting measurements of cellular Na^+ responses at physiological temperatures. Loading of ANG-AM in brain slices resulted in a specific staining of astrocytes with little background fluorescence, meaning that contamination of the fluorescent signal by remaining extracellular dye was not an issue. Moreover, any dye leaking from cells would be saturated by high extracellular $[Na^+]$ and thus contribute marginally to measured intracellular responses. Loading of ANG-AM in vivo was not tested in this study. However, it is likely that it will give successful staining by using either bulk loading with a procedure similar to the one we used for acute slices (Hirase et al., 2004), or by injecting a bolus the dye with a glass pipette in the area of interest (Garaschuk et al., 2006b; Stosiek et al., 2003). The former technique is likely to lead to a preferential staining of astrocytes when the later will give a homogeneous loading of both astrocytes and neurons.

Emission and excitation spectra were measured on ANG-filled astrocytes or neurons to optimize imaging parameters. Determination of intracellular spectra is essential as cellular environment can significantly alter spectral properties as compared to the in vitro situation. Indeed, excitation and emission maxima in situ were slightly higher than mentioned by the manufacturer from in vitro calibration data. Excitation maximum was 532 nm, a significantly higher wavelength than usual "fluorescein-like" green emitting probes. Emission spectrum was also redwards shifted with a maximum at about 550 nm. These unusual excitation and emission wavelengths mean that the imaging equipment needs to be specifically tuned to get an optimal signal. In wide-field

microscopy, we used a monochromator to illuminate at the excitation maximum and collected light through a long-pass emission filter. More selective detection could be obtained with an "eosin" band-pass filter centered at 550 nm. Nevertheless, because of the bright fluorescence of the dye, high quality measurements could be done with suboptimal filter combinations. With a confocal microscope, detection can be optimized by the use of spectral detection to pick the appropriate emission wavelength range. However, laser lines available on most confocal microscopes do not match perfectly ANG excitation profile. We got satisfactory results with 488 nm or 514 nm lines of an argon laser. We also checked whether ANG is suitable for two-photon microscopy. The dye was actually excited by a femtosecond Ti:Sapphire laser over a broad range of near-infrared wavelengths, with a maximum at 790 nm. This means that ANG can be used for high resolution imaging in thick brain slices or in whole animal during behavior.

Calibration of Na^+ sensitivity was done as for the spectra in cells loaded with ANG to take into consideration possible interference of cell constituents with measurements. ANG responded to steps of $[Na^+]$ with gradual increases in fluorescence in the 0-50 mM range, encompassing usual $[Na^+]$ observed during physiological responses (Fleidervish et al., 2010; Jaffe et al., 1992; Rose and Konnerth, 2001; Rose et al., 1999). The calibration curve followed a hyperbolic function similar to a Michaelis-Menten kinetics as was previously shown for SBFI (Rose et al., 1999). This downward shift of the calibration curve was attributed to the indicator saturation rather than to a reduction in fluorescence intensity induced by Na^+-dependent cell-swelling since similar calibration procedure performed with ratiometric dye SBFI did not evidence any significant volume change. The apparent K_d 38.7mM was higher than for SBFI (26 mM) (Rose et al., 1999) but still in a useful range for intracellular responses. It means that ANG is especially well suited to measure Na^+ in small cell compartments such as axons, dendrites or dendritic spines were Na^+ transients typically reach 10 to 40 mM (Rose and Konnerth, 2001; Rose et al., 1999). ANG exits in 2 versions: ANG-1 and ANG-2. Experiments in this study were performed with ANG-1. ANG-2 is a similar molecule to ANG-1 and has similar molecular weight, brightness and spectral properties. Both versions differ only in their Na^+ sensitivity: ANG-2 has a lower apparent K_d than ANG-1, meaning that it is better suited for studies in large cell compartments with small Na^+ increases, like the neuron soma. The absence of shift in the fluorescence emission profile for different $[Na^+]$ indicate that unlike SBFI, ANG can not be used for ratio imaging.

ANG detected pharmacologically-induced Na^+ responses in cultured astrocytes by activating Na^+-coupled glutamate uptake or blocking Na^+/K^+ATPase. To get a better assessment of the dye's performance in a neurophysiological setting we imaged canonical Na^+ responses in neurons. Whole-cell patch-clamp was used to precisely control neuronal responses and produce well calibrated stimuli. ANG did not alter basic electrophysiological properties of neurons, indicating that this dye is not significantly cytotoxic and that it is unlikely to interfere with neuronal functions. In the soma, Na^+ currents underlying action potential generation generated small fluorescence changes and single spikes could not be detected. This is similar to what was shown with SBFI (Fleidervish et al., 2010). The main explanation is that in the soma only small $[Na^+]$ changes occur during action potentials (Hodgkin and Huxley, 1952). In addition $[Na^+]$ decreases fast by diffusion in other cell compartments or the patch pipette (Fleidervish et al., 2010). In dendrites, fast Na^+ influx occurring during the backpropagation of action potentials was readily detected owing to higher amplitude Na^+ transients in small cell compartments (Fleidervish et al., 2010; Rose et al., 1999). Accordingly we expect ANG to be of great interest to study other neuronal subdomains like dendritic spines and the axon initial segment where Na^+ changes are essential. Inhibition of fluorescent transients by TTX, a blocker of voltage-gated Na^+ channels, indicates that ANG specifically detects Na^+ and does not respond to K^+, the other main monovalent cation present in the intracellular environment. Measurement of AMPA-induced Na^+ transients simultaneously by electrophysiology and ANG fluorometry allowed comparing estimates of $[Na^+]$ changes obtained with both methods. The value obtained from the electrophysiology was slightly higher than the value expected from fluorescence measurements. We attribute this to the fast diffusion on Na^+ in the cell and to its buffering by the patch pipette (Meier et al., 2006). Finally we show that ANG can be selectively loaded in astrocytes in brain slices and that glutamate transporter dependent Na^+ responses can be observed. This property will make ANG the indicator of choice to demonstrate neuron-astrocyte metabolic coupling (Magistretti, 2006) and the propagation of astrocytic metabolic waves (Bernardinelli et al., 2004) in intact networks.

ANG was designed to overcome the limitations of existing Na^+ dyes. This new molecule is based on the design of SBFI and uses a diaza crown ether to bind Na^+. The main difference with SBFI is the attachement of a new fluorophore group (personal communication from Dr Akwasi Minta). This new fluorophore gives ANG a visible excitation range and a greatly improved brightness as

compared to SBFI. Excitation with visible light brings better imaging conditions than UV excitation used for SBFI, resulting in deeper tissue measurements and lower phototoxic damage. The greater fluorescence change when binding Na^+ explains that small responses can be detected with a higher signal to noise ratio than with SBFI and also means that lower illumination might be used to detect them. Better deep tissue imaging, higher signal to noise ratio, and lower intensity visible light illumination make ANG a much better dye than SBFI to image in brain slices or in vivo. A safer mode of illumination is especially important since some essential physiological mechanisms, as intercellular astrocytic calcium waves, are inhibited by excessive illumination (Kuga et al., 2011). Another great advantage of ANG over SBFI is that it could be used to follow Na^+ responses induced by UV photolysis of caged compounds. ANG is also superior to other visible Na^+ dyes produced so far. Unlike Sodium Green it retains a high Na^+ sensitivity when loaded into cells and its response is not significantly altered by binding to intracellular content. As compared to CoroNa Green, it has a much longer intracellular retention time and does not leak significantly from cells during experiments.

Conclusions

ANG is a novel Na^+ indicator with attractive characteristics including (i) a homogeneous and stable cytosolic loading, (ii) excitation in the visible spectrum as well as with 2-photon, (iii) absence of significant cytotoxicity, (iv) an almost linear dependency of fluorescence on Na^+ concentration in the range of usual physiological responses, (v) a high efficiency of Na^+ detection allowing accurate measurement of Na^+ events, especially in small cellular compartments, (vi) kinetic parameters allowing the recording of fast sodium transients, (vii) effective bulk-loading of the cell permeant form for studying astrocytic functions. It will bring substantial improvements to Na^+ imaging of brain function, especially for deep tissue and in vivo applications.

Acknowledgements

References

Bernardinelli, Y., Azarias, G., Chatton, J.Y., 2006. In situ fluorescence imaging of glutamate-evoked mitochondrial Na+ responses in astrocytes. Glia 54, 460-470.

Bernardinelli, Y., Magistretti, P.J., Chatton, J.Y., 2004. Astrocytes generate Na+-mediated metabolic waves. Proc Natl Acad Sci U S A 101, 14937-14942.

Chatton, J.Y., Marquet, P., Magistretti, P.J., 2000. A quantitative analysis of L-glutamate-regulated Na+ dynamics in mouse cortical astrocytes: implications for cellular bioenergetics. Eur J Neurosci 12, 3843-3853.

Cossart, R., Ikegaya, Y., Yuste, R., 2005. Calcium imaging of cortical networks dynamics. Cell Calcium 37, 451-457.

Despa, S., Vecer, J., Steels, P., Ameloot, M., 2000. Fluorescence lifetime microscopy of the Na+ indicator Sodium Green in HeLa cells. Anal Biochem 281, 159-175.

Fleidervish, I.A., Lasser-Ross, N., Gutnick, M.J., Ross, W.N., 2010. Na+ imaging reveals little difference in action potential-evoked Na+ influx between axon and soma. Nat Neurosci 13, 852-860.

Garaschuk, O., Milos, R.I., Grienberger, C., Marandi, N., Adelsberger, H., Konnerth, A., 2006a. Optical monitoring of brain function in vivo: from neurons to networks. Pflugers Arch 453, 385-396.

Garaschuk, O., Milos, R.I., Konnerth, A., 2006b. Targeted bulk-loading of fluorescent indicators for two-photon brain imaging in vivo. Nat Protoc 1, 380-386.

Gobel, W., Helmchen, F., 2007. In vivo calcium imaging of neural network function. Physiology (Bethesda) 22, 358-365.

Helmchen, F., Imoto, K., Sakmann, B., 1996. Ca2+ buffering and action potential-evoked Ca2+ signaling in dendrites of pyramidal neurons. Biophys J 70, 1069-1081.

Hirase, H., Qian, L., Bartho, P., Buzsaki, G., 2004. Calcium dynamics of cortical astrocytic networks in vivo. PLoS Biol 2, E96.

Hodgkin, A., Huxley, A., 1952. A quantitative description of membrane current and its apllication to conduction and excitation in nerve. J Physiol 117, 500-544.

Jaffe, D.B., Johnston, D., Lasser-Ross, N., Lisman, J.E., Miyakawa, H., Ross, W.N., 1992. The spread of Na+ spikes determines the pattern of dendritic Ca2+ entry into hippocampal neurons. Nature 357, 244-246.

Kang, J., Arcuino, G., Nedergaard, M., 2005. Calcium Imaging of Identified Astrocytes in Hippocampal Slices. In: Yuste, R., Konnerth, A. (Eds.), Imaging in neuroscience and development: a laboratory manual. Cold Spring Harbor Laboratory Press, Cold Spring Harbor, pp. 290-297.

Kuga, N., Sasaki, T., Takahara, Y., Matsuki, N., Ikegaya, Y., 2011. Large-Scale Calcium Waves Traveling through Astrocytic Networks In Vivo. J Neurosci 31, 2607-2614.

Lasser-Ross, N., Ross, W.N., 1992. Imaging voltage and synaptically activated sodium transients in cerebellar Purkinje cells. Proc Biol Sci 247, 35-39.

Magistretti, P.J., 2006. Neuron-glia metabolic coupling and plasticity. J Exp Biol 209, 2304-2311.

Meier, S.D., Kovalchuk, Y., Rose, C.R., 2006. Properties of the new fluorescent Na+ indicator CoroNa Green: comparison with SBFI and confocal Na+ imaging. J Neurosci Methods 155, 251-259.

Minta, A., Tsien, R.Y., 1989. Fluorescent indicators for cytosolic sodium. J Biol Chem 264, 19449-19457.

Neher, E., Augustine, G.J., 1992. Calcium gradients and buffers in bovine chromaffin cells. J Physiol 450, 273-301.

Nimmerjahn, A., Kirchhoff, F., Kerr, J.N., Helmchen, F., 2004. Sulforhodamine 101 as a specific marker of astroglia in the neocortex in vivo. Nat Methods 1, 31-37.

Rose, C.R., Konnerth, A., 2001. NMDA receptor-mediated Na+ signals in spines and dendrites. J Neurosci 21, 4207-4214.

Rose, C.R., Kovalchuk, Y., Eilers, J., Konnerth, A., 1999. Two-photon Na+ imaging in spines and fine dendrites of central neurons. Pflugers Arch 439, 201-207.

Rose, C.R., Ransom, B.R., 1996. Intracellular sodium homeostasis in rat hippocampal astrocytes. J Physiol 491 (Pt 2), 291-305.

Rose, C.R., Ransom, B.R., 1997. Regulation of intracellular sodium in cultured rat hippocampal neurones. J Physiol 499 (Pt 3), 573-587.

Sorg, O., Magistretti, P.J., 1992. Vasoactive intestinal peptide and noradrenaline exert long-term control on glycogen levels in astrocytes: blockade by protein synthesis inhibition. J Neurosci 12, 4923-4931.

Stosiek, C., Garaschuk, O., Holthoff, K., Konnerth, A., 2003. In vivo two-photon calcium imaging of neuronal networks. Proc Natl Acad Sci U S A 100, 7319-7324.

Stuart, G.J., Sakmann, B., 1994. Active propagation of somatic action potentials into neocortical pyramidal cell dendrites. Nature 367, 69-72.

Szmacinski, H., Lakowicz, J.R., 1997. Sodium Green as a potential probe for intracellular sodium imaging based on fluorescence lifetime. Anal Biochem 250, 131-138.

Figure legends

Figure 1 Intracellular characterization of ANG. (a) Fluorescence image of primary astrocytes loaded with ANG-AM. Scale bar, 30 μm. One- (b) and two- (c) photon excitation spectra (see also Fig. S1). (d) Emission spectra measured at different $[Na^+]_i$ in situ. (see also Fig. S1) (e) Calibration curve obtained by plotting peak amplitude of emission spectra against $[Na^+]$. Data are mean ± s.e.m. (n=10 cells). Dotted line is the hyperbolic fit to the data. (f) Typical astrocytic Na^+ responses induced by glutamate and ouabain application (n=6 cells).

Figure 2 Neuronal Na^+ responses. (a) Fluorescence image of a layer 2/3 pyramidal neuron patched with ANG-containing electrolyte. (b) Top: Fluorescence responses to trains of depolarization measured at the soma and their inhibition by TTX. Number of trains below traces. Arrowhead, time of stimulus. Bottom, left to right: sample train of 10 action currents, superimposed single fluorescence traces of 3 consecutive responses to 2 AC trains, superimposed averaged responses to 1 (clearer) to 5 (darker) AC trains. (c) Average fluorescence responses normalized to the maximal response plotted against AC number. Red line, linear fit. Data are mean ± s.e.m. (n=4 cells). (d) 3D reconstruction of a patched neuron. Red line shows linescan position on apical dendrite. (e) Dendritic fluorescence transients recorded during backpropagation of action potentials (top). Space over time display of the matching linescan recording (bottom). (f) Averaged dendritic responses to 10 (left) and 20 (right) AP trains (top). Sample AP trains (Bottom). (g) Representative sequence of fluorescence responses to AMPA puffs of different durations (indicated above) and inhibition by CNQX (top). Voltage-clamp traces simultaneous to fluorescence responses presented above (bottom). Arrowhead, time of puff during CNQX application. (h) Averaged AMPA currents amplitude (blue) and fluorescence peak amplitude (red) dependence on puff duration. Diamonds, CNQX; Triangles 15 min washout; Squares, washout 30 min. Data are mean ± s.e.m.(n=4cells) (i) Individual fluorescence values plotted against corresponding AMPA current amplitude. Red line, linear regression (n=49 points). Scale bars, 30 μm.

Figure 3 Bulk loading of astrocytes in slices. (a) Fluorescence image of astrocytes double stained with sulforhodamine 101 (left panel) and ANG (center panel). Scale bar, 30 μm.

Magnification of an ANG stained astrocyte (right panel). Scale bar, 5 μm. (b) Sample trace of astrocytic fluorescence response to glutamate puffs of increasing durations. (c) Dependence of astrocytic Na+ response to puff duration in control condition (●) and after inhibition by TFB-TBOA (100nM, ○). Lines are linear fits to the data.
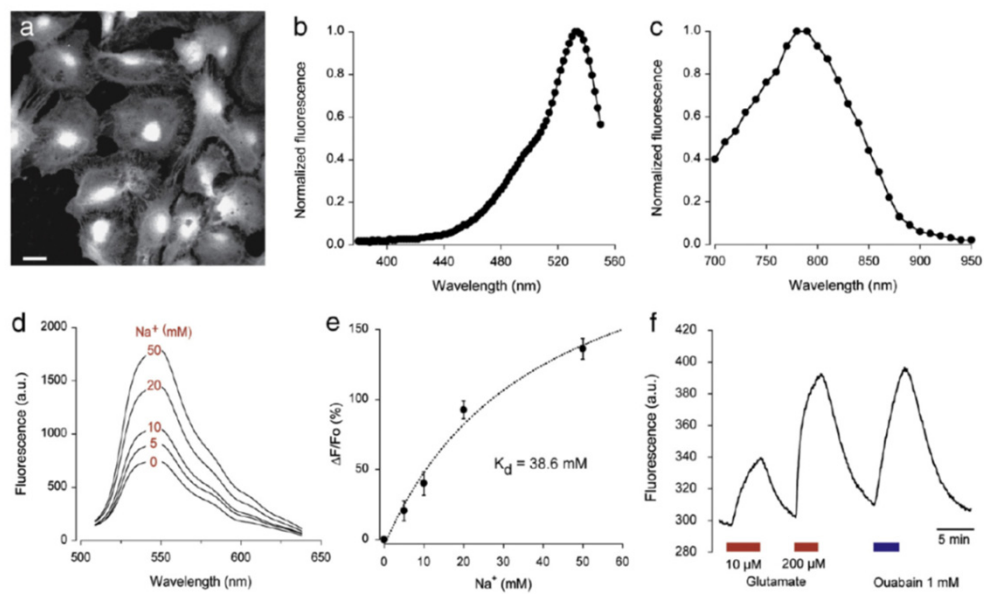
Figure 1

a

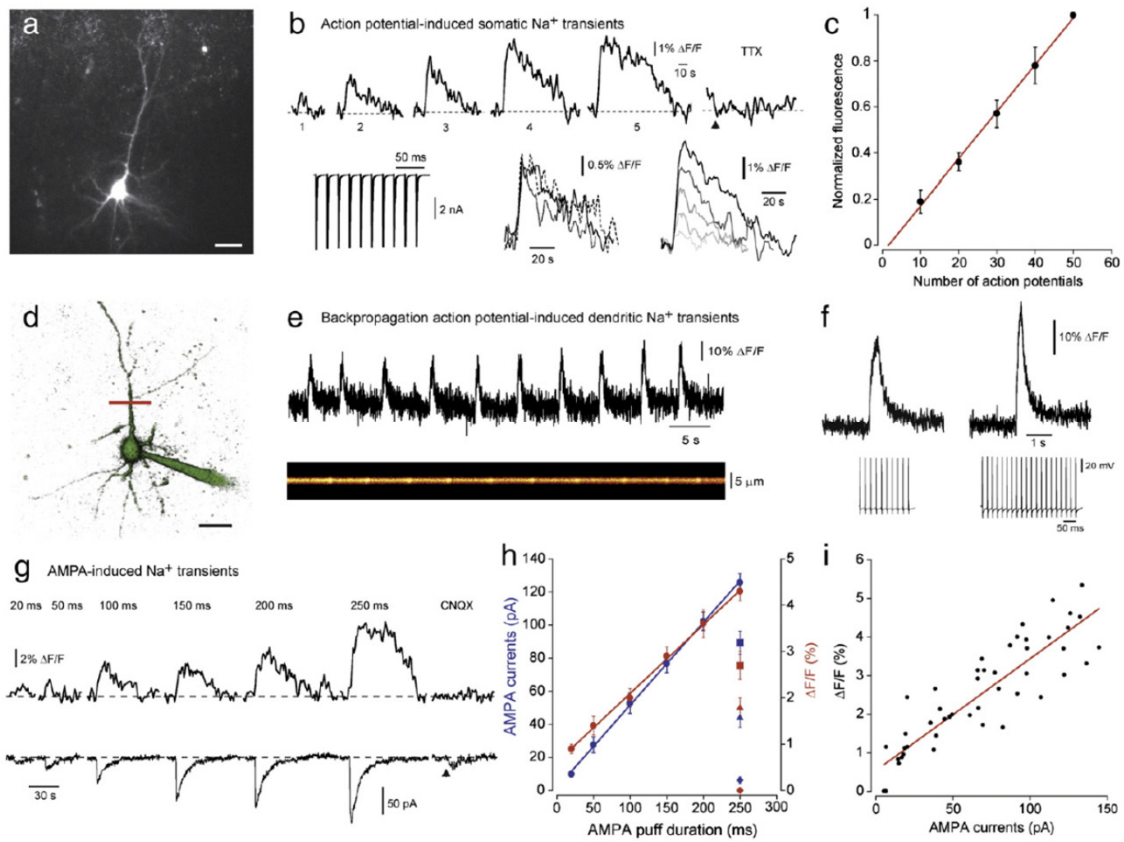**b** Action potential-induced somatic Na⁺ transients

1% ΔF/F
10 s
TTX

1 2 3 4 5 ▲

50 ms
2 nA

0.5% ΔF/F

20 s

1% ΔF/F
20 s

c

Normalized fluorescence

Number of action potentials

d

e Backpropagation action potential-induced dendritic Na⁺ transients

10% ΔF/F
5 s
5 µm

f

10% ΔF/F
1 s
20 mV
50 ms

g AMPA-induced Na⁺ transients

20 ms 50 ms 100 ms 150 ms 200 ms 250 ms CNQX

2% ΔF/F

30 s ▲ 50 pA

h

AMPA currents (pA)
ΔF/F (%)
AMPA puff duration (ms)

i

ΔF/F (%)
AMPA currents (pA)

Figure 2

a   Sulforhodamine 101   Asante Natrium Green

b   2% ΔF/F

Glu 50   100   150   200   250   30 s

c

ΔF/F

Glutamate puffs duration (ms)

Figure 3